

In-situ TEM observations of abnormal grain growth, coarsening, and substrate de-wetting in nanocrystalline Ag thin films

Rand Dannenberg^{a,*}, E.A. Stach^b, J.R. Groza^c, B.J. Dresser^c

^aBOC Coating Technology, 2700 Maxwell Way, Fairfield CA 94533 0252, USA

^bNational Center for Electron Microscopy, Lawrence Berkeley Lab, Berkeley CA, USA

^cDepartment of Chemical Engineering/Materials Science, University of California at Davis, CA, USA

Received 15 July 1999; received in revised form 3 November 1999; accepted 3 November 1999

Abstract

Abnormal grain growth is studied in nanocrystalline sputtered Ag films. Eighty nanometer thick Ag films are DC sputter deposited onto back-etched amorphous silicon nitride membranes. Specimens are annealed in a heating stage in an in-situ TEM for various temperatures and hold times. With the same specimen, we proceed to higher temperatures after the apparent halt of growth for sufficiently long hold times. The grain size distribution of the as-deposited films is bi-modal, with large abnormal grains with 100 nm diameters, embedded in a matrix of smaller grains of 15 nm diameters. Coarsening begins at temperatures of approximately 100°C, and quickly reaches a plateau. The growth process restarts only after sufficient temperature increases, and plateaus at each succeeding temperature. Using a variation of the Mullins–Von Neumann law, the activation energy for the abnormal growth is found to be 0.274 eV, consistent with the value reported for pore formation during electromigration via surface diffusion in Ag. Grain growth appears to stop above temperatures of 350°C, eventually leading to triple junction pore formation at 350°C and de-wetting of the film from the substrate at 600°C. The de-wetting is the high temperature limit of the thermal grooving which cancels the driving force for grain growth at the lower temperatures. TEM images as evidence of this effect are presented, along with observations on the pore formation that support surface diffusion as the mass transport mechanism for grooving, pore formation, and as the limiting mass transport mechanism for the grain growth. © 1999 Elsevier Science S.A. All rights reserved.

Keywords: TEM; Substrate de-wetting; Nanocrystalline Ag thin films

1. Introduction

Silver is used as the infrared reflective layer in thin film optical coatings, such as low-emissivity and solar control systems for heat rejection or retainment, and for high reflectance mirrors in the visible spectrum. For some processes, it would be desirable to heat treat a silver layer or multilayer after its deposition, with minimal degradation of the metals optical or mechanical properties. Since it oxidizes slowly, silver is also a desirable material for fundamental studies in which the films must be deposited ex-situ to the observation tool, and undergo exposure to air.

In this work, we study the effect of post-deposition vacuum annealing on the nanocrystalline microstructure of DC sputtered silver films. This is of fundamental interest, as it is unclear what the limiting diffusion mechanism should be for grain coarsening. The large surface area of the thin film form could make surface diffusion and related effects

dominant, or owing to the large grain boundary area per unit volume from the nano-grains, perhaps the limiting mass transport mechanism is grain boundary diffusion. Bulk diffusion seems unlikely at the temperatures of interest, 400°C or lower.

Electromigration experiments with silver films with grain sizes on the order of microns place the activation energy of pore formation to be between 0.3 and 0.43 eV at temperatures between 160 and 213°C [1,2]. The mass transport was concluded to be surface diffusion in these cases. At higher temperatures, 225–280°C, the activation energy rises to 0.95 eV attributed to grain boundary diffusion [1]. At temperatures greater than 650°C in bulk specimens, the activation energy reported is 1.89 eV, determined from tracer diffusion. [3].

We will measure the activation energy for coarsening and grain growth by the method of in-situ TEM vacuum annealing of DC sputtered Ag films, noting additional qualitative behavior supporting our findings.

Mullins has described a mechanism for the promotion of abnormal grain growth (also called secondary grain growth

* Corresponding author. Tel.: + 1-707-423-2244.

E-mail address: rand.dannenberg@ct.boc.com (R. Dannenberg)

or secondary recrystallization) in films, due to specimen thickness effects. He proposes that grain boundaries of large, many-sided grains, pinned at the surface by thermal grooves may break away from the grooves if the surface energies of the grains in contact are sufficiently different [4]. This type growth may result in near uniform fibertexture. Normal growth may also be inhibited by particles of secondary phases and precipitates, where grain growth is initially normal but becomes abnormal in the later stages as the precipitates form [5–8].

In nanocrystalline copper, palladium and silver compacts, room temperature abnormal grain growth has been observed, where the activation energy for the copper grain growth was 0.8 and 1 eV for unoxidized silver [9]. Nanocrystalline silver compacts have shown abnormal growth at 100–200°C, and nickel at 80°C [10–12]. For nanocrystalline copper grain growth, reduced values of the activation energy have been reported at 0.3 eV (30 kJ/mol), over a factor of two lower than what has been reported for polycrystalline (not nanograined) material [13]. This suggests different mass transport mechanisms may be at work for different grain sizes. In addition, this value is lower than that of 0.8 eV for nanocrystalline copper grain growth in Ref. [9], so there is some disparity in the literature.

Trace oxygen has been shown to slow the process of sintering and grain growth in DC sputtered copper nanoparticles. [14,15]. For slightly oxidized nano-crystalline silver compacts (7 at.%O), the activation energy for grain growth is twice that of pure nanocrystalline silver, at 1 eV for the latter and 2 eV for the former. This was measured using Kissinger analysis of DSC results [9].

2. Experimental

Films were DC sputter deposited to a thickness of 80 nm in an ILS in-line sputtering system built by BOC Coating Technology. Typical base vacuum was 10^{-6} Torr, with an argon pressure of 3 mTorr. The linear power density was 2.8 kW/817 mm. The target to substrate distance was 4". Film thickness was measured with a Detak profilometer.

The substrate for the in-situ TEM experiments were 3 mm diagonal (2.2 mm per side) back-etched silicon wafers with a silicon nitride amorphous membrane, which fit into a standard 3 mm TEM stage. The viewable area was 470×470 μm . Specimens were sputtered the night before transportation to the TEM and stored in high vacuum overnight.

The in-situ TEM was a JEOL 200 CX with LaB₆ filament running at 200 keV. The heating stage was capable of reaching temperatures of 1300°C, and could be ramped to any temperature in under 60 s.

The heating experiment was carried out as follows: beginning at 100°C, specimens were held at temperature for times varying between 5 and 10 min. The specimen was then cooled, and micrographs were taken. The temperature was then re-ramped to 100°C for an additional hold time. The

process is repeated at that temperature until no obvious changes occur. The temperature is then increased. Films were analyzed at temperatures of 100, 200, 300, and 350°C. No further microstructural changes were observable after reaching equilibrium during the 350°C treatment until about 600–700°C when pores began to develop, and unoxidized films de-wet the substrate. The temperature is measured on the specimen stage *adjacent* to the sample.

The effect of beam heating was investigated by two simple methods. One method involved heating the specimen to 100°C for a sufficient hold time until the growth stopped, observing a fixed area with the beam fully saturated. The beam was then quickly moved onto other areas not previously exposed, and held there. No further growth under the beam was observed. This was repeated with other specimens at temperatures of 125, 150, 175, 200, 300, 350, 600, and 700°C. In a second method, an Ag film was surface oxidized over several weeks in air. The surface oxide seems to block surface and/or grain boundary diffusion paths, and prevents the de-wetting of the film from the substrate until the melting point (961°C). This is consistent with a doubling of the activation energy for grain growth in slightly oxidized Ag [9], where for our case, the oxidation also prevented grain growth until 400°C. The film de-wets at an indicated temperature of 960°C with the beam fully saturated. Since the melting point should be dominated by the bulk of the film (un-oxidized silver), we may interpret this as the beam heating having negligible effect on the indicated melting point of the material. This establishes also that the thermometer is properly calibrated, and correctly indicates the specimen temperature.

NIH image was used to extract the size distributions from scanned-in micrographs. For the abnormal grains, 20 kX images were used. For the small (and numerous) 'normal' background matrix of grains, 100 kX images were used for more accurate measurements of their sizes, and, to prevent the tendency to count only the large grains viewable at 20 kX. NIH image calculates the *areas* of the grains. We have converted the areas to diameters before the calculation of mean diameters.

3. Data and analysis

Fig. 1 shows the results of the analysis of the abnormal grains. The mean grain diameters of the normal regions are 14 nm for the as deposited, 26 nm for the 100°C annealed films, 74 nm for the 200°C anneals, 84 nm for 300°C, and 90 nm for 350°C. We shall refer to these sizes as D_n (or R_n where a radius is indicated). The D_n values were determined from the endpoint of the anneals at the various temperatures, since little or no change could be observed (in-situ) in the background after the first anneal time-increment at each temperature.

Fig. 2 shows the histograms used for the quantitative analysis. Fig. 3 shows characteristic micrographs associated

with the curves of Fig. 2. As can be seen, the distribution in each case is bi-modal. The areas investigated at 20 and 100 kX are not the same. The small diameter peak corresponding to the *normal* background indicates the correct size (D_n), but, the height of the peak may not be compared to that of the larger abnormal peak. The mean diameters of the particles in those peaks were used for the quantitative analysis, to follow.

From Fig. 1, it can be seen that there is an obvious plateau in the growth of the abnormal grains for each hold temperature. The abnormal growth process restarts with a sufficient increase in the temperature, noting from the transition from 100–200°C, 200–300°C, and 300–350°C. This can be partially explained by the pinning of grain boundaries by thermal grooving as per Mullins [4,16].

We will now explain our method of analysis of the grain growth before proceeding. Thermal grooves form since a grain boundary can reduce its total surface free energy by shrinking in a direction normal to the film surface. Mullins has shown that a grain boundary with a catenoid shape will be immobilized when the angle of the groove with the film surface θ_g becomes greater than the angle of the boundary with the film normal, given by a monotonically increasing function $f(h/R)$, where h is the film thickness and R is the radius of curvature of the boundary at the film surface. When $f(h/R) > \theta_g$, the boundary may break free from the notch, as to do so results in a decrease of its area. For $f(h/R) < \theta_g$ the boundary would have to increase its surface area to move away from the notch. For a film held at a fixed temperature where the grooves have reached an equilibrium shape, undergoing grain growth, this condition will eventually be met, and boundary motion will cease.

Evidence of grooving is seen in Fig. 4. A deeply grooved grain boundary may be seen in which parts of it have extended to the substrate. The high temperature limit of the thermal grooving is to cause the film to de-wet the substrate, and form individual islands in the solid state

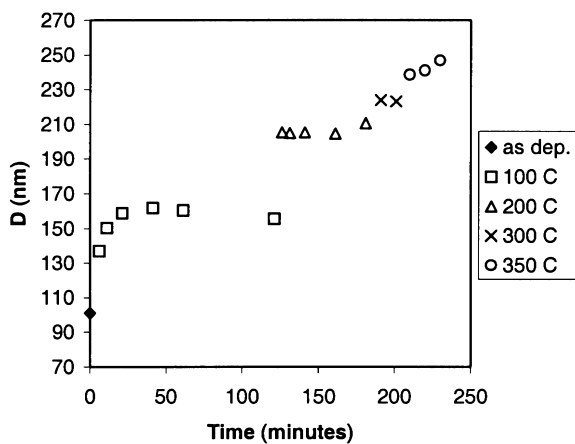


Fig. 1. Results of analysis using NIH image to measure the average diameters of the abnormal grains. Lines through the plateaus show which points were averaged for computing the derivative (Eq. (2)).

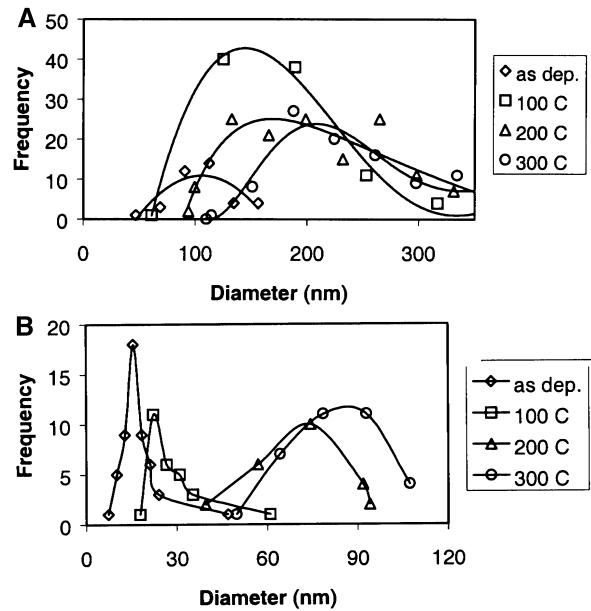


Fig. 2. (a) Abnormal grain diameter distribution of the specimen at the endpoint stages of the anneals at the indicated temperatures. 20 kX images were used for the data reduction. Sixth order polynomials are used only to show the trends in the data. The peaks of these trend lines are *not* used in the activation energy calculation. *Average* grain size is used for all the kinetic calculations. (b) Grain size distribution for the normal matrix grains. 100 kX images were used for the data reduction. Since the areas of the normal and abnormal analyses are different, the peak heights of the two cases cannot be fairly compared. Again, *average* grain sizes are used in the calculation of the activation energy.

(Fig. 5). The qualitative evidence given in the discussion supports groove formation via surface diffusion, and not by an evaporation process.

How can the growth process restart on an increase in temperature? Why doesn't the growth process restart after cooling and reheating to the same temperature (for our case, after cooling rapidly for photographs). This is not so easily explained in terms of the Mullins theory. The authors postulate that a sudden rapid rise in temperature causes the forces to go into a temporary state of non-cancellation. There is a time delay on returning to equilibrium during which grain growth may continue. We may express this as

$$F_{\text{tot}} = 2\gamma/R - F_{\text{gr}}(t, \tau, T) \quad (1)$$

Where F_{tot} is the total driving force on a grain boundary, $2\gamma/R$ is the driving force for grain growth due to its surface energy and radius of curvature, and $F_{\text{gr}}(t, \tau, T)$ is the opposing force associated with the grooving, $\tau(T)$ is a time delay that is dependent on the temperature. When $F_{\text{tot}} = 0$, grain growth stops. We will return to the topic of the nature of this force in the discussion.

An estimation of the activation energy for the abnormal grain growth is possible from the from the points in Fig. 1, which correspond to the restart of the growth process, provided $2\gamma/R \gg F_{\text{gr}}(t, \tau, T)$. This is most likely to occur

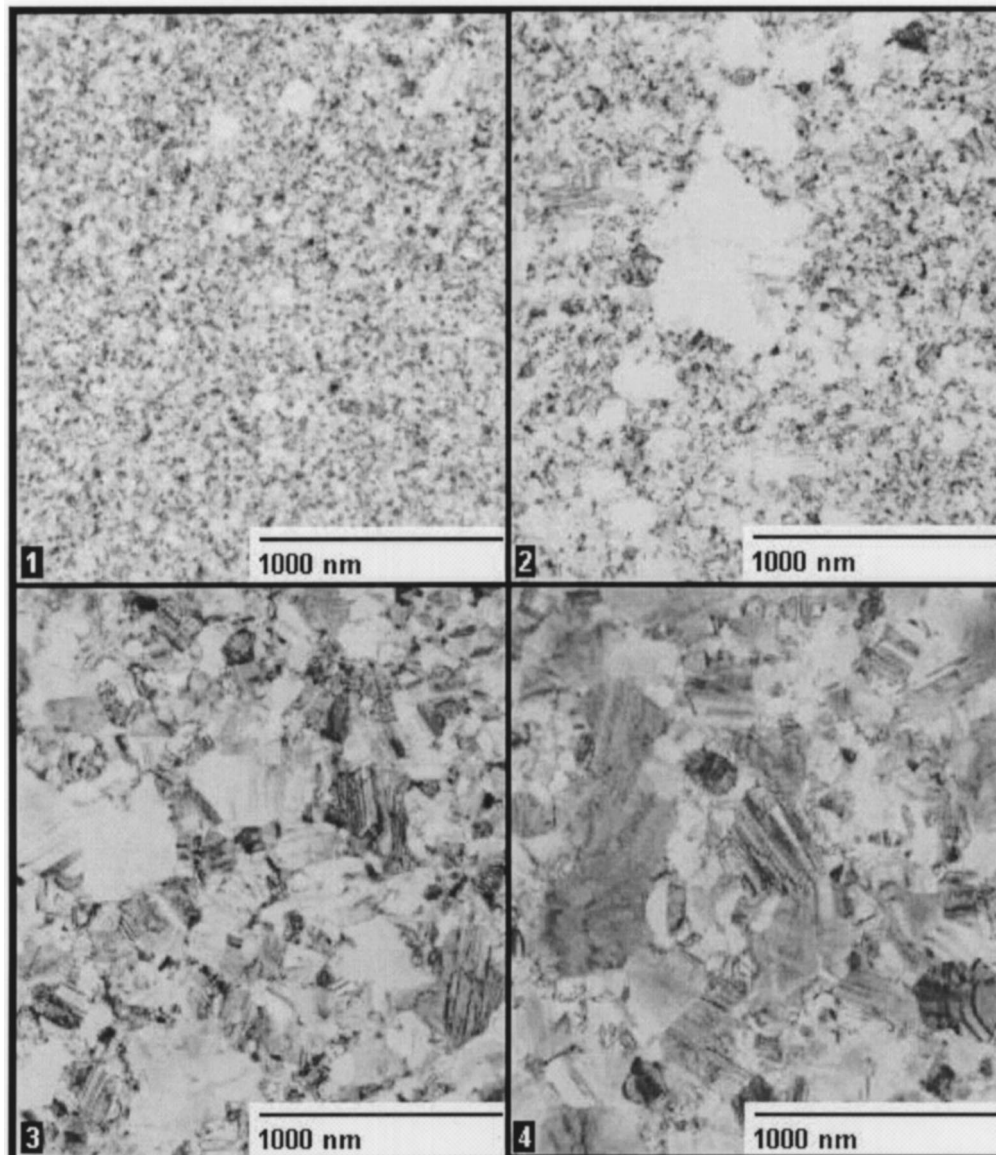


Fig. 3. Portions of the 20 kX TEM images analyzed in Fig. 2. These are the endpoints in time of each hold temperature. (1) As deposited. (2) 100°C. (3) 200°C. (4) 300°C.

right after the jump to a higher temperature as boundaries escape from grooves.

Consider an *abnormal* grain with radius R_a embedded in a background matrix of *normal* grains with radius R_n . We may expect the large abnormal grain to have many sides. For a near circular abnormal grain, if $R_a \gg R_n$, then the number of sides of the abnormal grain is approximately $N_a = \pi R_a / R_n$. The rate of increase of the diameter of the large grain is driven by the radius of curvature of the surrounding small matrix grains in contact with it. The large grain is expected to have many more than six sides. Since force equilibrium at the triple junctions demands that the angles between grain boundaries be 120° , the sides of the large grain (viewed from its center) are convex, therefore, the force on the boundaries will be directed radially outward from the center of the large grain. Therefore, large grains will have the

tendency to grow and consume the smaller surrounding grains. The radial velocity of the large grain is then given by the product of the *grain boundary* mobility times the total force on the boundaries, $M(T)F_{\text{tot}}(t, \tau, T)$. The growth law may then be written for times *immediately* after the temperature change as

$$dR_a/dt = (1/6)M(N_a - 6)\gamma/R_n \quad (2)$$

This is a simple variation of the Mullins–Von Neumann growth law, but applied to the abnormal grains. Note that as R_n approaches R_a the grains are competing on more equal ground. The approximation mentioned for N_a is then no longer valid, and the classic growth law $dA/dt = (\pi/3)k(T)(N - 6)\gamma$, where A the grain area, is recovered. It has been pointed out that if the grain boundary velocity is

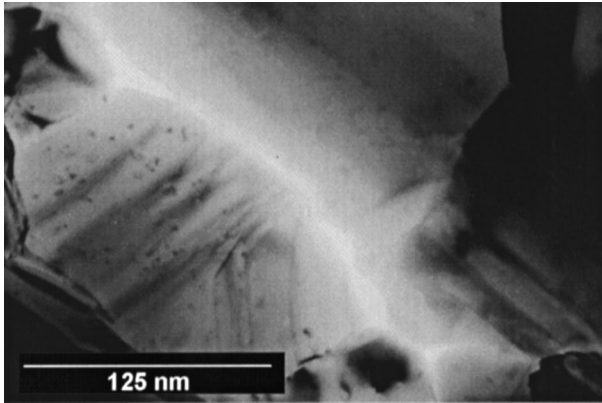


Fig. 4. Deeply grooved grain boundary in which parts have reached the substrate, 400°C. The long low-contrast area running from the upper left to the lower right is the amorphous silicon nitride membrane onto which the films were deposited (between the two large central grains).

discontinuous, which is often the case in grain growth inhibited by thermal grooving, the latter equation, and hence Eq. (2), cannot be applied [17]. Its application is assumed to be valid for $2\gamma/R \gg F_{gr}(t, \tau, T)$, and this is taken up in the discussion.

More conventional growth laws cannot be applied to these data, for several reasons. First, the usual growth laws are such that for any temperature, growth should *never* actually stop, merely slow down for sufficiently long hold times. Therefore, these laws cannot formally account for the plateau. For example, consider the law $dR/dt = k/R^n$, where the value of n is taken from best fits to the curvature of D vs. *time* data [18]. The effect of grooving on the analysis using this law would be to yield artificially high values of n , since this assumes the driving force falls only due to average grain size increases. For example, applying this law to the first four points of the 100°C anneal data yields $n = 11$, high value in comparison to studies on other nanocrystalline systems where $n \sim 5$ [19]. Second, the sudden jumps in D lack the D (or R) vs. *time* curvature necessary to deduce fitting variables, at the higher temperatures. Third, the growth is abnormal.

Table 1 shows the values used for extraction of the activation energy. The derivative in Eq. (2) is estimated from

Table 1
Data used for computing the mass transport activation energy from Eq. (2)

Time (min)	Temp (°C)	D_a (nm) ^a	dR/dt (nm/min)	D_n (nm)	N_a	$\gamma M(T)$ (nm ² /min)
0	As deposited	101		14	22.7	
7	100	137	2.57			6.429
121	100	159		26	19.2	
125	200	206	5.9			34.62
181	200	206		74	8.75	
191	300	223	0.85			71.45
201	300	223		84	8.37	
208.5	350	242	1.26	90 ^b		133.43

^a Calculated from the average value of the plateau.

^b From 350°C endpoint. Not involved in the derivative calculation.

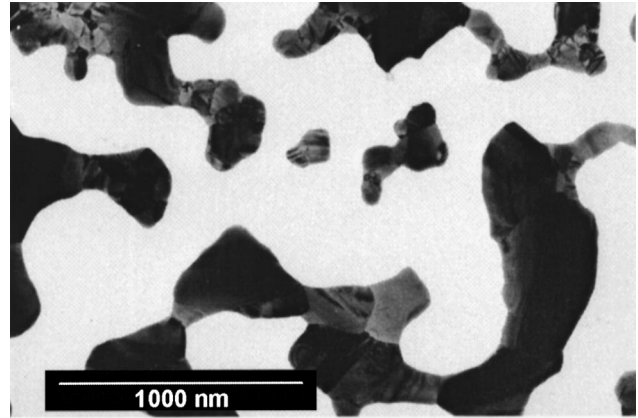


Fig. 5. Film that de-wetted the substrate in the solid state at 615°C.

the pairs of entries in Table 1, indicated in boldface and plain text. The activation energy is computed by the usual method (Fig. 6).

Assuming that the grain boundary mobility has the form $M(T) = (A/T) \exp(-Q/kT)$, we deduce an activation energy of $Q = 0.274$ eV, consistent with surface diffusion from the electromigration damage studies on silver [1], and that of nanocrystalline copper [13]. Assuming a grain boundary energy of 0.5 J/m², $A = 4.189 \times 10^{-5}$ cm⁴-K/J-s. If $A = D_0 l^2/k$ where the number of atoms per unit area $l^{-2} = 1.5 \times 10^{19}$ m⁻², we deduce $D_0 = 8.67 \times 10^{-13}$ cm²/s.

4. Discussion

Mullins has pointed out that abnormal grains should not be impeded by thermal grooving, provided that the matrix grain diameters are sufficiently less than the film thickness, $R_n < h$. Since the matrix grains are providing the driving force for the network, it is the angle of matrix grain boundaries with the surface normal which will dictate whether normal or abnormal growth occurs. According to the estimates of Mullins, $\theta_g = \gamma_0/6\gamma_s = 3^\circ$ where $\gamma_{b,s}$ are the boundary and film surface tensions [4]. Further, a catenoid matrix grain with $h/R_n > 1$ will have an angle greater than 17° , thus, abnormal growth should *not* be impeded by groov-

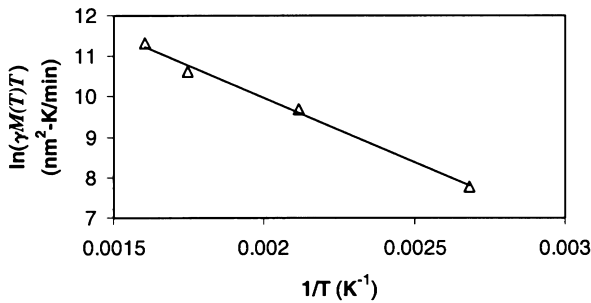


Fig. 6. Linear relation of the data of Table 1, yielding an activation energy of 0.274 eV.

ing. These estimates were made using data extracted from materials with grain sizes on the order of millimeters and temperatures close to the melting point, and may not be wholly applicable to our observations on nanocrystalline films at temperatures far below T_{melt} .

In the 100°C anneal, abnormal growth does persist for longer time periods at that temperature, and $h/R_n \sim 8$, so the plateau at this temperature is an unexpected result in view of the estimates of Mullins, under the above mentioned conditions. For the higher temperature anneals, all growth stops abruptly. The plateau seems more reasonable, since h/R_n decreases to 2.7 at 100°C to 1.14 at 200°C, to 0.95 at 300°C, and 0.88 at 350°C. Conditions in these films are such that the growth of both matrix and abnormal grains are impeded, as evidenced by the observation that *all* growth halts, for extended observation periods in the in-situ TEM, and, in the image analysis.

Observing the growth in-situ allows us to comment on several qualitative features that are consistent with our quantitative treatment. It has been reported that grain boundaries in freeing themselves from thermal grooves grow in sporadic stop/start spurts [4]. This can occur when conditions permit the interiors of a pinned grain boundary to migrate and curve, until the boundary angle with the normal is greater than the critical angle and it escapes from the notch. This is certainly consistent with what has been observed in our specimens: the individual boundary velocities are *not* smoothly varying functions of time.

We have also noted on occasion that once a boundary has made a sudden sporadic move, there is a cascade-like event in which boundaries in the vicinity will also move, suggesting that there is some local interaction between them. An isolated groove perturbs the surface of the film for considerable distances, and the nanocrystalline grain sizes may cause these perturbations to overlap. According to the Mullins theory, the surface perturbation from a groove exponentially decays to a flat surface with decay constant $3d/(\gamma_0/\gamma_s)$, where d is the groove depth [4]. Consider the grooves demonstrated to reach the substrate with $d = h = 80$ nm, $(\gamma_b/\gamma_s) = 1/3$. Taking conservatively 3 decay constants as the distance at which the surface is effectively flat, the

grooves could interact over distances of $9h = 720$ nm, which is large compared to the grain sizes under investigation. When one boundary escapes from its groove, the surface changes disrupt the equilibrium of surrounding grooves, ‘stimulating’ the escape of other boundaries, and so on, in a cascade effect. The effect can be propagated to large distances from the original boundary. In addition, once a boundary has abandoned a groove, there is a ‘healing time’ in which the surface flattens, so the interaction due to a changing surface may persist for a finite duration. This would further support the observation of jumps in grain sizes with large temperature changes, since one grain escaping from its groove due to a transient condition would have long range effects on a number of other boundaries. This interaction would influence the $\tau(T)$ in the force opposing grain growth, F_{gr} .

Boundaries escaping from grooves have been shown to leave depressions (from incomplete healing) in the film surfaces where they were once pinned. In the in-situ TEM, most of the grains of our specimens show contrast similar to a dense twin structure, which may be related to groove abandonment and healing time, which can be on the order of hours.

The force F_{gr} must be temperature and time dependent. The Mullins standard theory results in a solution for the static groove whose *shape* is independent of time and temperature. The shape is dependent on the angle θ_g (given by force equilibrium) requiring $\gamma_0 = 2\gamma_s \sin(\theta_g)$ from the static theory [16]. Therefore, according to this theory, if the surface tensions do not change, θ_g is fixed for all time and temperature, and so sudden growth associated with a temperature dependent groove angle change is not predicted by this model. However, higher temperatures and therefore mobilities may permit the internal regions of a few grain boundaries (that are pinned at the surface) to migrate to angles greater than θ_g , escape from their grooves, and stimulate growth elsewhere via the groove interaction cascade.

The theory for a groove–boundary system translating due to a *constant* driving force has a velocity which goes as $V \sim B(T)/d^3$ [4]. $B(T)$ is related to the *atomic* mobility. The shape of the groove system in this theory is also independent of time and temperature. For surface diffusion $d = 0.973 \tan(\theta_g) (B(T)t)^{1/4}$ [4]. Therefore, a moving groove–boundary system can decelerate with time and temperature. The force F_{gr} therefore has both dynamic components that increase with time, and statistical components, since some boundaries may be completely immobilized by grooves, while others are not.

Again, Mullins theory assumes that the surface tensions are independent of temperature. If the ratio γ_b/γ_s should decrease on increased temperature (either temporarily or permanently) θ_g would decrease, permitting the escape of some boundaries, but, would increase on temperature reduction, which would be consistent with no observed growth on returning to the same temperature (or lower) after the

growth has stopped. On a temperature rise, once a number of grain boundaries have escaped from the grooves, for whatever reason, new grooves must form on the boundaries. Immediately after escaping, $d = 0$ so the boundaries are initially unimpeded, which justifies $2\gamma/R \gg F_{gr}$ on the temperature increase, and a temperature dependent time delay to the cancellation of the driving force for growth. The time delay is related to the time it takes for the depth of the new grooves to become significant enough to impede boundary motion.

We have calculated the activation energy for the mass transport to be 0.274 eV, which is consistent with earlier reported values for surface diffusion in Ag [1]. We have calculated this in a rather novel way, by estimating what is the *average* radial velocity of the abnormal grains immediately after the rise to higher temperatures. It is a discrete approximation. We cannot say exactly, during the first time increment, when the growth process stops on going from 100 to 200°C, from 200 to 300°C, and on to 350°C. For the latter temperature, the associated value of N_a is only 8.37, so the use of Eq. (2) to higher temperatures would be of questionable validity, and so was not pursued. Nevertheless, the surface diffusion conclusion is consistent with the in-situ observation of the early stages of the pore formation.

Our estimate of 0.274 eV is low compared to the DSC estimates of powder compacts that have yielded 1 eV, however, those were not film specimens, and this analysis method does not allow the differentiation between abnormal and normal growth processes. Also, this difference is of about the same size as the disparity between activation energies for grain growth in nanocrystalline copper, 0.8 and 0.3 eV of Refs. [9,13]. Different methods of preparation and analysis result in different activation energies.

Fig. 7 shows an early stage pore showing a wide surrounding area of what is obviously thinner material. The early pores develop at triple junctions, but, the thinning is not restricted to the area of the boundaries of the triple

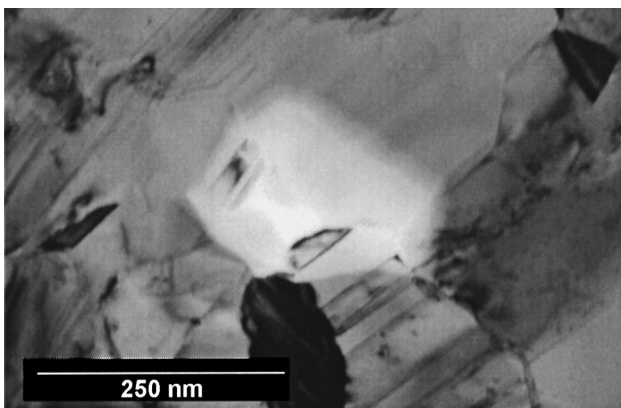


Fig. 7. Thermally grooved grain boundary junction that has reached the substrate, 600°C. Note the large thinned area surrounding the pore, which is not restricted to the triple junctions or their boundaries. This suggests that the mass transport is neither grain boundary diffusion or an evaporation process, but surface diffusion.

junction. This is indicative of depletion predominantly by a surface diffusion mechanism. The solid state de-wetting of the film, the end result of which is shown in Fig. 5, is clearly a surface diffusion mechanism, where material moves from areas on the bead near the substrate to the surface of the film, a sensible limit of the early stage pore development described. The isolated beads flow smoothly as material moves towards their centers of curvature, resulting in an obvious thickening of the film as evidenced by intensity reduction in the microscope. Also, films held at the temperatures in which the catastrophic de-wetting occurs do not eventually disappear, but form static, isolated islands. The latter observation therefore excludes an evaporation process.

Given this qualitative data, a consistent interpretation of this 0.274 eV activation energy is now possible. The atomic mechanism involved in the motion of the grain boundaries consists of atomic jumps across the interface from one crystallite to another. This is expected to occur with an activation energy between 0.75 and 1.25 eV, more consistent with grain boundary diffusion. Since this is a thin film specimen, boundary motion and grain growth can be inhibited by the formation of thermal grooves which pin the boundaries at the film surface. The thermal grooves form by surface diffusion, and surface diffusion should have an activation energy ~ 0.3 eV. Given that the activation energy for grain boundary diffusion is larger than surface diffusion, grain boundary diffusion increases faster with temperature. The boundary motion then becomes limited by the formation of thermal grooves which form because of surface diffusion. Groove-boundary systems may also translate with steady state velocities via a surface diffusion mechanism [4]. Our analysis method simply returns the activation energy of the limiting mass transport mechanism.

The authors had wished to calculate the time required at a given temperature for a groove in an 80 nm thick film to reach the substrate, using the Eq. (3) [16]. This necessitates the diffusion coefficient to be extracted from the grain boundary mobility, and hence the D_0 value. The value returned for the pre-exponential, $D_0 \sim 10^{-13}$ cm²/s, is an extremely low value, seven orders of magnitude lower than values reported for surface diffusion [4,20].

It was thought that the cause of this low value was due to inaccurate measurement of the time to reach the new grain diameter plateau after incrementing to a new temperature. As a check of this, it was assumed that the derivative in Eq. (2) was computed without error for the 100°C anneal, as this anneal showed curvature. The time to reach the plateau for the 350°C anneal was reduced from 7.5 min to the artificially low value of 0.1 min. The duration for which grain growth occurred was certainly longer than this. The other data points were ignored in calculating Q and D_0 . This leads to the result $Q = 0.61$ eV and $D_0 = 4 \times 10^{-8}$ cm²/s. These are maximum possible values. The Q is still indicative of surface diffusion, and the D_0 is still two to three orders smaller than expected values. This demonstrates that the

mechanism indicated by the activation energy, using our method, seems sensitive only to the grossest errors in the measurement of the times.

At this time, we can offer no satisfactory explanation for this low value of the diffusion coefficient, although there are a number of possibilities we cannot substantiate. (1) Inapplicability of Eq. (2), since boundary velocity may be too discontinuous as a function of time. (2) Boundary curvature is not restricted to the film surface. (3) Surface oxidation has lowered the jump frequency. (4) The *grain boundary* mobility is not simply related to the diffusion coefficient for such a system.

Using the diffusion coefficients determined by our analysis, we have calculated the groove depth as a function of time according to the equation

$$d(T, t) = 0.973 \tan(\theta_g) \left(\frac{D(T)}{kT} \frac{\Omega^2}{l^2} \gamma t \right)^{1/4} \quad (3)$$

which is for a groove formed by a surface diffusion mechanism [16]. Ω is the atomic volume. θ_g is taken to be 6° . After 10 min at the melting point of 961°C , the predicted depth is only 0.5 nm. The 80 nm film is observed to de-wet the substrate at 615°C . The small depths returned are due to the low value of the extracted diffusion coefficient.

5. Conclusions

In 80 nm thick sputtered Ag films, abnormal grain growth is limited by the formation of thermal grooves by surface diffusion, as evidenced quantitatively by a 0.274 eV activation energy, mass transport at temperatures $\sim 100^\circ\text{C}$, and by qualitative observations of the process of pore formation and de-wetting.

Abnormal grain diameters plateau at each hold temperature. Abnormal growth can be impeded by thermal grooving if the matrix grains are sufficiently large compared to the film thickness. Mullins estimate that if $R_n < h$ abnormal growth should *not* be impeded by thermal grooving seems to be consistent with only with the early stages of the 100°C anneal. Perhaps a more reasonable way to state the conditions for unimpeded abnormal growth is that $f(h/R) \gg \gamma_b/\gamma_s$.

The restart of the growth process only on increases to higher hold temperatures calls for more detailed understanding of how a groove approaches its new equilibrium shape on changes in temperature. The authors postulate that a rise in temperature above one where a system has reached equilibrium allows some boundaries to internally migrate to angles greater than the groove angle, so that some boundaries may escape from their grooves. The grooves in nanocrystalline films are closely spaced. An order of magnitude calculation suggests surface perturbations can overlap and interact over distances larger than the nanocrystalline grain diameters, so that the motion of one boundary perturbs the state of another boundary groove-system, and non-local growth proceeds via a cascade effect. Related to this is the

need to experimentally establish whether the groove angle changes, either temporarily or permanently, on temperature changes.

Activation energies indicative of the mass transport mechanism can be reduced from jumps in the average grain diameter for sufficiently small time increments after the increase to higher hold temperatures.

The diffusion coefficients (D_0 values) returned by our method are seven orders of magnitude smaller than published values. The cause of this is in need of more investigation.

Grain growth is a ‘many-interface’ problem. The motion of one boundary affects another. Growth laws such $F \sim 1/r$ with no opposing terms do not account for many body interactions in grain boundary networks, or predict stagnation of grain growth growth in a formal manner.

6. Further work

We are presently carrying out a detailed analysis of the growth kinetics of the matrix grains by conventional methods, to which these results will be compared. Cross sectional specimens are also being prepared for observation in the TEM and FE-SEM at the National Center for Electron Microscopy, to understand how thermal grooves approach their equilibrium shapes on temperature changes, and interact.

Acknowledgements

We wish to thank BOC Coating Technology for supporting this work, specifically Dr Peter Tausch. Thanks to the National center for Electron Microscopy for continued access to the microscopes. Thanks to Professor Alexander King, Head of the Department of Materials Science at Purdue for helpful discussions on thermal grooving, abnormal growth, and stereology.

References

- [1] R.E. Hummel, H.J. Geier, Thin Solid Films 25 (1975) 335.
- [2] R. Rosenberg, L. Berenbaum, Atomic Transport in Solids and Liquids, Verlag der Zeitschrift für Naturforschung, Tubingen, Germany, , p. (1971) 113.
- [3] R. Weast, -68, CRC Handbook of Chemistry and Physics, 58th ed., CRC Press, Boca Raton, FL, 1977, pp. F68.
- [4] W.W. Mullins, Acta. Metall. 6 (1958) 414.
- [5] P. Hai, C.V. Longworth, Thompson, J. Appl. Phys. 69 (1991) 3929.
- [6] S.C. Mehta, D.A. Smith, U. Erb, Mat. Sci. Eng. A204 (1995) 227.
- [7] G. Ramanath, H.Z. Xiao, L.C. Yang, A. Rochet, L.H. Allen, J. Appl. Phys. 78 (1995) 2435.
- [8] C. Cabral, J.M.E. Harper, K. Halloway, D.A. Smith, R.G. Schad, J. Vac. Sci. Tech. A10 (1992) 1706.
- [9] B. Gunther, A. Kimpmann, H.D. Kunze, Scr. Metal. Mater. 27 (1992) 833.
- [10] T. Kizuka, H. Ichinose, Y. Ishida, J. Mat. Sci. 32 (1997) 1501.
- [11] V.Y. Gertsman, R. Birringer, Scr. Metal. Mater. 30 (1994) 577.

- [12] U. Erb (in a personal communication to the author of Reference 6).
- [13] S.K. Ganapathi, D.M. Owen, A.H. Chockski, *Scr. Metal. Mater.* 25 (1991) 2699.
- [14] D.L. Olynick, J.M. Gibson, R.S. Averback, *Appl. Phys. Lett.* 68 (1996) 343.
- [15] L. Dierdre, J. Olynick, Murray Gibson, Robert S. Averback, *Mat. Sci. Eng. A204* (1995) 54.
- [16] W.W. Mullins, *J. Appl. Phys.* 28 (1957) 333.
- [17] M.A. Palmer, M.E. Glicksman, K. Rajan, *Acta. Mater.* 46 (1998) 6397.
- [18] T.R. Malow, C.C. Koch, *Acta. Mater.* 45 (1997) 2177.
- [19] L.Z. Zhou, J.T. Gou, *Scr. Mater.* 402 (1999) 139.
- [20] N. Gjostein, *Diffusion*, ASM, Metals Park, OH, , p. (1973) 271.